

Chapter 6

Establishing the CRISPR-Cas9 technology in primary human T cells

6.1 Introduction

As an unbiased approach pooled genome-wide CRISPR screens have lead to many novel discoveries (Doench, 2017; Shalem et al., 2014; Wang et al., 2014a). In such genome-wide screens, cell lines are usually transduced with a lentivirus to introduce Cas9 stably into the cells and a genome-wide sgRNA lentiviral library. Cells containing Cas9 and sgRNAs are then selected using antibiotics prior to phenotypic screening (Doench, 2017). Cells with the phenotype of interest are isolated and the sgRNAs that cause the phenotype are determined by sequencing (Doench, 2017). Performing such a screen in primary T cells would be of immense interest in order to improve understanding of how the response of T cells to target antigen is regulated at the genetic level. For example, this could lead to progress in using T cells to target cancers by immunotherapy.

Several researchers have taken the approach of performing genome-wide screens in cancer cell lines in order to identify cancer genes that affect T cell killing (Pan et al., 2018; Patel et al., 2017). These type of screens have identified new immunotherapy targets, or mechanisms of cancer resistance to immunotherapy. However the findings may be specific to the cell lines used and may not always reflect complex cancer biology in vivo. Performing screens in primary T cells could increase the possibility of finding a broadly applicable strategy for improving T cell mediated killing of tumours.

While pooled genome-wide screens can be performed in immortalised cancer cell lines,

this approach is more challenging in primary T cells for several reasons. Firstly, pooled screens usually require large cell numbers (10s of millions) (Doench, 2017). Secondly, a selection procedure for cells that have incorporated Cas9 and sgRNAs after lentiviral transduction is required. This can be in the form of antibiotic selection or sorting by FACS. The selection procedure can take several weeks, and therefore cannot be used on cells with a limited life span in vitro (Doench, 2017), such as mouse T cells. However, primary human T cells in theory fit the required criteria. They are able to survive for many months in tissue culture by regular re-stimulation using PHA and irradiated buffycoat from allogeneic donors. Through re-stimulation, they can also be expanded to give the desired amount of cells. Furthermore, any findings in primary human T cells could have immense medical potential.

An early study trying to use CRISPR in primary human T cells revealed transfection difficulties when nucleofecting plasmids encoding Cas9 and sgRNAs, leading to low CRISPR efficiency (Mandal et al., 2014). Nucleofecting human T cells with Cas9-RNPs has been more successful (Schumann et al., 2015), but this approach only allowed targeting a select set of genes, rather than unbiased, genome-wide screening.

One option to enable a genome-wide screen would be to produce human T cells that stably express Cas9. This could be achieved by transducing human T cells with a lentiviral vector encoding Cas9, however lentiviral vectors containing large inserts (the *Cas9* gene is ~4000 bp in size) often result in low viral titre (Doench, 2017; Ramezani and Hawley, 2002; Sanjana et al., 2014). This chapter describes my efforts to test CRISPR in human T cells and to produce primary human T cells that stably express Cas9 using lentiviral transduction. Such cells would provide the possibility to generate stable KOs in primary human T cells. Perhaps such cells could even be used for a genome-wide screen in primary human T cells using the same approach of a pooled genome-wide lentiviral sgRNA library commonly used in cell lines.

6.1.1 Chapter aims

- Transduce hCTL with a lentivirus encoding Cas9 as well as antibiotic resistance or a fluorescent marker to be able to select successfully transduced cells.
- Test nucleofection of hCTL and the transient Cas9-RNP CRISPR approach (optimised in chapter 3) in primary hCTL.

- Compare the stable (Cas9 lentivirus) and transient (Cas9-RNP) approaches in terms of CRISPR efficiency.

6.2 Results

6.2.1 Transduction of hCTL with Cas9-Blast lentivirus

Initially hCTL were transduced with the Cas9-Blast lentivirus (Sanjana et al., 2014), encoding Cas9 separated by a 2A sequence derived from porcine teschovirus (P2A) from a gene encoding resistance to the antibiotic blasticidin. Therefore, any cells that express Cas9 upon transduction could be selected by treatment with blasticidin. In order to be able to select transduced cells, it was first necessary to establish what concentration of blasticidin killed all untransduced cells, which can vary greatly between cell types (Doench, 2017). Therefore, I tested the blasticidin sensitivity of hCTL by exposing them to a variety of blasticidin concentrations over a time period of 15 days. Blasticidin was renewed every two days and viability measured by flow cytometry. Changes in cell morphology as detected by forward scatter/side scatter analysis and staining with DAPI were used as an indicator of whether cells were alive or dead. 5 $\mu\text{g/ml}$ was determined as the lowest blasticidin concentration that I tested that killed all hCTL within 15 days of treatment, as live cells were still remaining after 15 days treatment with 1 $\mu\text{g/ml}$ blasticidin (Figure 6.1). Therefore, 5 $\mu\text{g/ml}$ Blasticidin was used to select hCTL transduced with the Cas9-Blast lentivirus.

As a control for transduction, hCTL were transduced with a lentivirus encoding just the fluorescent protein GFP in parallel to transduction with the Cas9-Blast lentivirus. 44.5% of the cells were successfully transduced with the GFP lentivirus, as visualised by flow cytometry (Figure 6.2A), confirming that there was no technical problem during the transduction process. No band corresponding to Cas9 was detected by WB using lysates derived from hCTL transduced with Cas9-Blast lentivirus, in contrast to lysates from Cas9 hom mice which served as a positive control for the Cas9 protein (Figure 6.2B). However, Cas9 could be detected by WB after transduction of HEK293T cells with the Cas9-Blast lentivirus (Figure 6.2C). This indicated low transduction efficiency with this lentivirus in hCTL, but not in HEK293Ts. PCR was used as a more sensitive technique to show that the Cas9 lentivirus had successfully integrated in some hCTL (Figure 6.2D). DNA isolated from transduced HEK293T (positive control) was run alongside DNA from hCTLs on the agarose gel. It is noteworthy that while DNA was isolated from 450,000 hCTLs for the PCR reaction, the signal is lower than the signal generated by DNA derived from only 10,000 transduced HEK

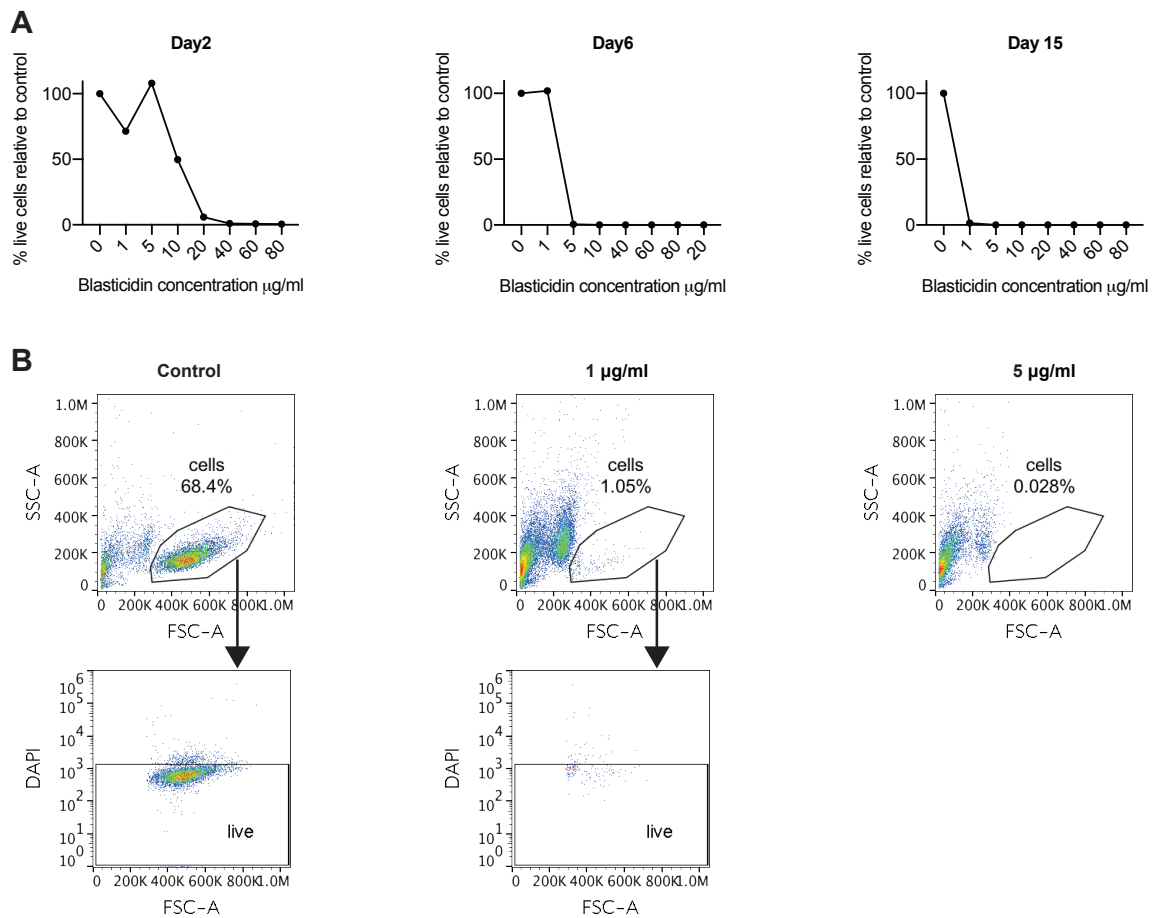


Fig. 6.1 Blastocidin concentration response. **A** Human T cells were treated with blasticidin at the indicated concentrations for 15 days. Blastocidin-containing media was renewed every 2-3 days. Viability was measured by gating on forward scatter (FSC) and side scatter (SSC) parameters by flow cytometry. The percentage of cells in the FSC/SSC gate was normalised to the treatment control (no blasticidin treatment) at each time point. **B** Representative flow cytometry plots after 15 days of blasticidin treatment showing the change in the FSC/SSC profile and the DAPI signal within the FSC/SSC gate.

cells. This confirmed that transduction of hCTLs with the Cas9-Blast lentivirus was much less efficient than transduction of HEK293T with the same lentivirus. Selecting the hCTLs in blasticidin almost killed transduced and untransduced cells to a comparable level after 6 days of blasticidin treatment (Figure 6.2E). Only a few live cells remained in the transduced samples, providing further evidence that the transduction efficiency was very low (Figure 6.2E). These live cells were sorted by FACS and single cell dilutions were performed in the hope to expand Cas9 expressing clones, but the cells did not grow subsequently.

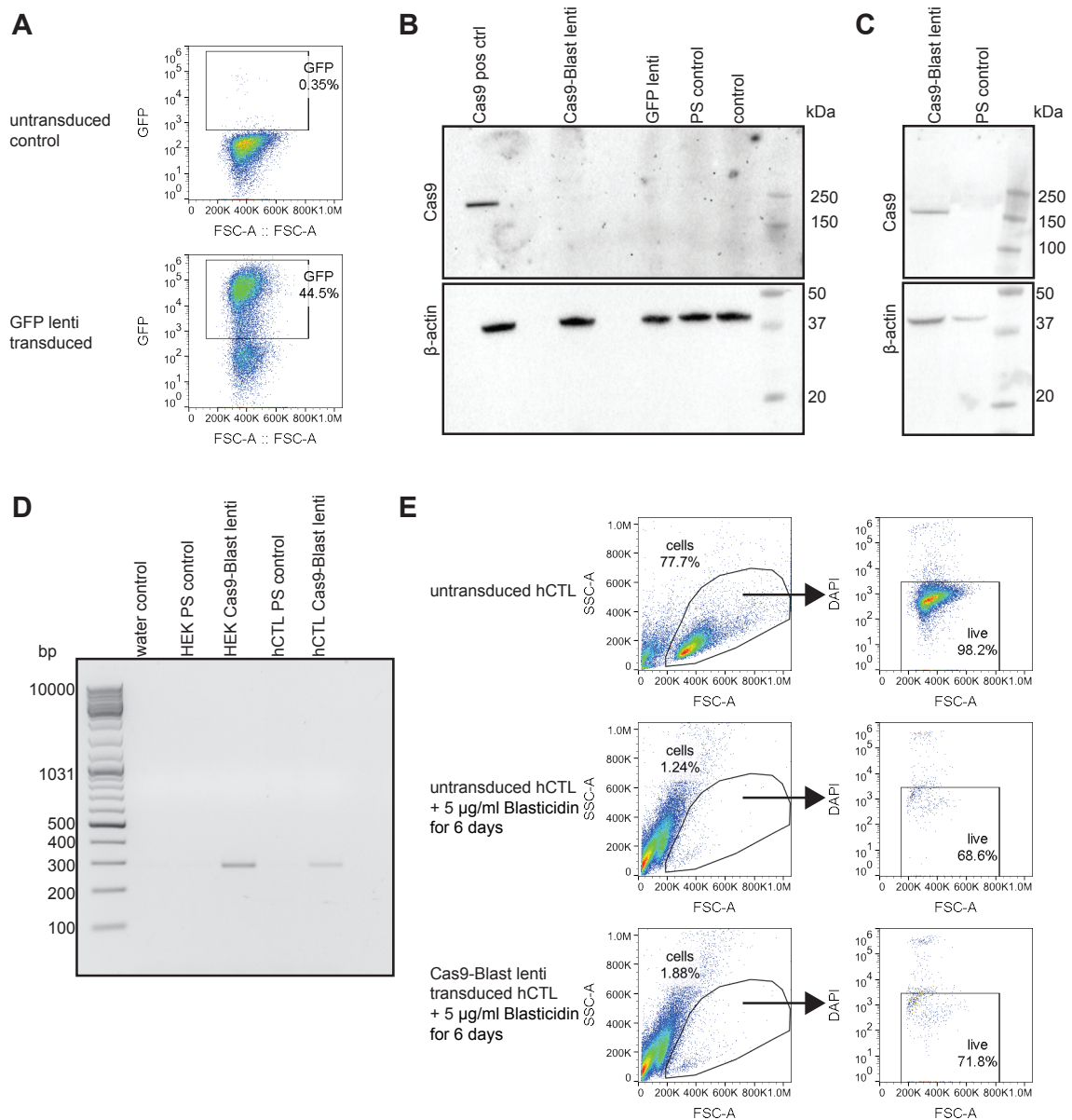


Fig. 6.2 Transduction of hCTL with Cas9-Blast lentivirus. **A** GFP expression profile of untransduced hCTL and hCTL transduced with pHRSIN-GFP lentivirus. **B** WB showing Cas9 protein expression in lysates derived from Cas9 hom mice (positive control), but not in samples transduced with Cas9-Blast lentivirus or any of the negative controls (samples transduced with a pHRSIN-GFP lentivirus, protamine sulfate (PS) treatment control samples, or untransduced control samples). **C** WB showing Cas9 protein expression in lysates derived from HEKs transduced with Cas9-Blast lentivirus, but not in PS treatment control samples. **D** Agarose gel of products from a PCR with primers spanning a 274 bp region between the 3' end of the Cas9 gene and the blasticidin resistance gene. **E** Viability of untransduced hCTL and hCTL transduced with Cas9-Blast lentivirus after 6 days treatment with 5 μ g/ml blasticidin. PS = protamine sulfate, HEK = HEK293T.

6.2.2 Generation of a lentivirus encoding Cas9 and a fluorescent tag

As an alternative approach to antibiotic selection, Cas9 can be co-expressed with a fluorescent marker, which allows to detect successfully transduced cells by flow cytometry (Doench, 2017). As hCTL were successfully transduced with the GFP lentivirus (pHRSIN-GFP) used in Figure 6.2A, the *Cas9* gene was cloned into a mCherry fluorescent protein encoding version of the pHRSIN plasmid (pHRSIN-mCh).

The approach taken to insert *Cas9* into the pHRSIN-mCh vector is outlined in Figure 6.3A. I generated two plasmids, in the first plasmid mCherry was immediately downstream of the *Cas9* gene, in the second plasmid the *Cas9* gene was linked to mCherry via a sequence encoding the self-cleaving P2A peptide, shown to have high cleavage efficiency in human cells (Kim et al., 2011). For simplicity, the P2A sequence is referred to as 2A for the remainder of this results section.

Primers were designed that amplify the *Cas9* gene from the Cas9-Blast lentiviral plasmid by PCR. The primers included sequences that overlap with the pHRSIN-mCh plasmid, as well as a XhoI RE site upstream of *Cas9* and a BamHI RE site downstream of *Cas9*. The resulting PCR products were run on a gel (Figure 6.3B) and purified. The recipient plasmid (pHRSIN-mCh) was cut with XhoI and BamHI RE, run on a gel and also purified. The resulting insert and recipient vector fragments were joined by Gibson assembly. After bacterial transformation and selection on ampicillin plates, 8 colonies were picked per plate and expanded. After DNA purification, the DNA from the various different colonies was subjected to a restriction digest with XhoI and BamHI. Running the products of the restriction digest on a gel allowed for the isolation of colonies that appeared to have the correct insert as indicated by the excision of a band corresponding to the *Cas9* gene in size (~4000 bp) (Figure 6.3C,D). Sanger sequencing carried out by Source Bioscience confirmed the correct sequence of DNA derived from colonies 1c and 2e, while DNA from colonies 1e and 2h contained point mutations. The entire *Cas9* gene and its flanking regions to the pHRSIN-mCh vector were sequenced. Figure 6.4 shows plasmid maps for the final pHRSIN-Cas9-mCh and pHRSIN Cas9-2A-mCh plasmids that were subsequently used for lentivirus production.

As a control to test these lentiviral plasmids, I transduced P815 cells, as this mastocytoma cell line is more easily transduced than primary human T cells. The mCherry signal was measured by flow cytometry, and Cas9 protein expression was confirmed by WB (Figure 6.5). While only one band corresponding to Cas9 was observed in the Cas9-mCh lentivirus transduced samples, two bands were observed in the Cas9-2A-mCh lentivirus transduced

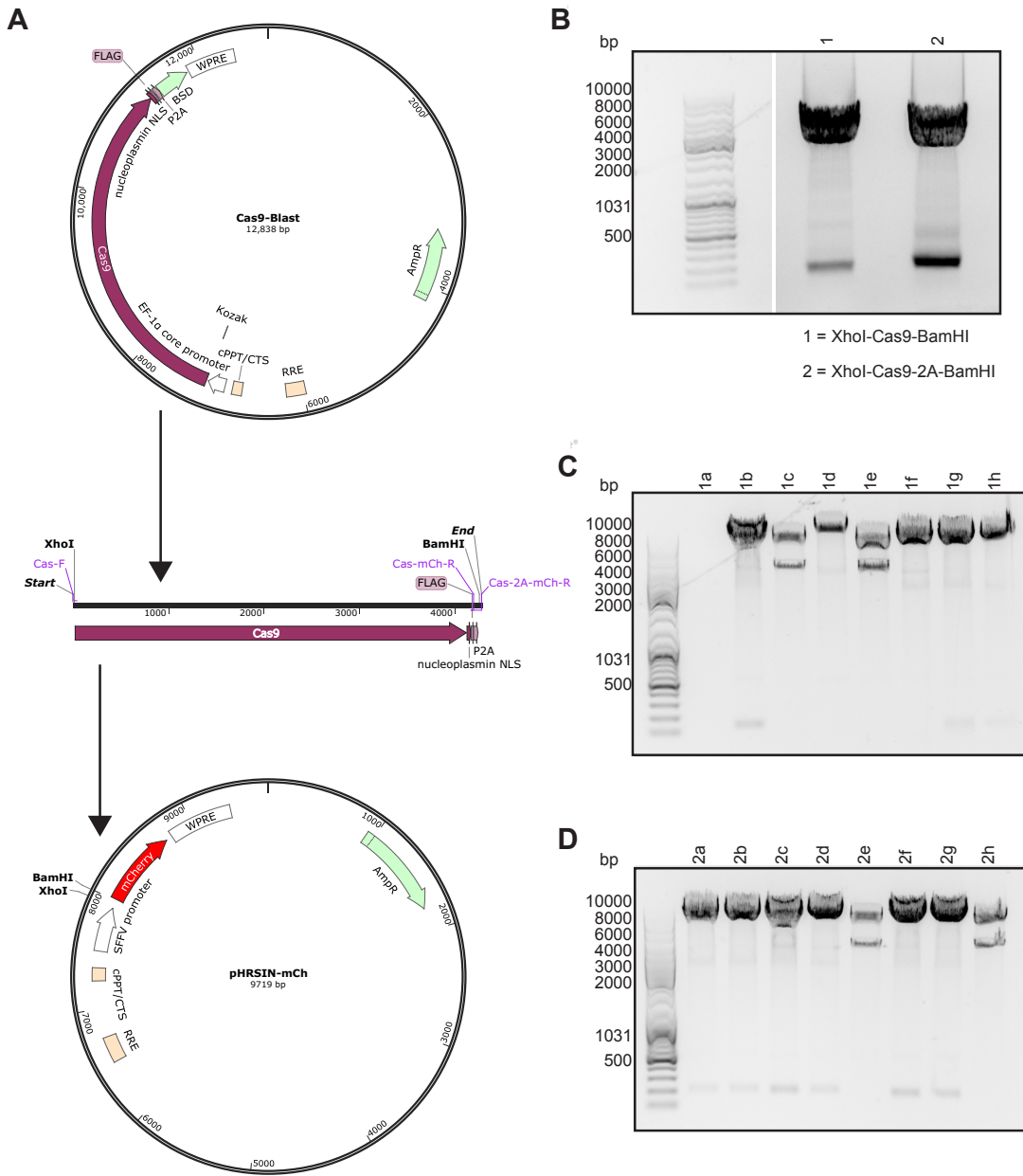


Fig. 6.3 Cloning Cas9 into the pHR SIN-mCh vector.

Fig. 6.3 Cloning Cas9 into the pHRSIN-mCh vector. **A** Schematic showing the plasmid map for the Cas9-Blast lentivirus (top) that acted as the source to amplify the Cas9 gene (middle) in order to insert it into the recipient plasmid pHRSIN-mCh (bottom). Location of the forward primer (Cas9-F) and reverse primers (Cas9-mCh-R and Cas9-2A-mCh-R) are indicated on the Cas9 gene (middle). Plasmid maps were created with snapgene. **B** Agarose gel showing Cas9 amplified from the Cas9-Blast plasmid using primers that add on a 5' XhoI restriction enzyme site and a 3' BamHI restriction enzyme site with (2) or without (1) the 3' 2A sequence. These PCR products were cloned into the pHRSIN-mCh vector digested with XhoI and BamHI restriction enzymes using Gibson assembly. **C and D** Agarose gels showing the banding pattern after using XhoI and BamHI restriction enzymes to digest the DNA derived from ampicillin-resistant clones (a-h) of NEB10beta bacteria that were transformed with the Gibson assembly products. DNA that showed the expected banding pattern, cutting out a ~4000 bp fragment corresponding to Cas9, were sequenced. RRE = rev response element, cPPT = central polypurine tract, SFFV = spleen focus forming virus promoter, EF1alpha = elongation factor 1alpha promoter, Cas9 = CRISPR-associated protein 9, NLS = nuclear localisation sequence, Flag = flag octapeptide tag, P2A = P2A self-cleaving peptide, BSD = blasticidin selection marker, WPRE = woodchuck hepatitis virus post-transcriptional regulatory element, AmpR = ampicillin resistance gene.

samples (Figure 6.5A). These two bands should correspond to two versions of Cas9, one where the 2A sequence successfully cleaved Cas9 from mCherry, and another where cleavage was not successful. Therefore, the higher MW band likely corresponded to Cas9 fused to mCherry, and the lower molecular weight band corresponded to Cas9 where the mCherry tag was cleaved. While this indicated that the 2A peptide was functional, I would have expected the 2A cleavage ability to be more efficient. However, to avoid any potential functional effects of tagging mCherry directly to Cas9, which may block Cas9 activity, the Cas9-2A-mCh lentivirus was used from now on.

Next, the Cas9-2A-mCh lentivirus was tested on two cell lines that are more closely related to hCTL than P815s: 1) Jurkat cells, a human T cell line, and 2) YT, a human NK cell line. Both cell lines were successfully transduced with the lentivirus as shown by the detection of mCherry signal by flow cytometry and detection of Cas9 by WB (Figure 6.6). Strikingly, the Cas9 expression was much stronger in the lentivirally transduced samples than in samples derived from Cas9 hom mice (described in chapter 3) (Figure 6.6B). While only faint bands corresponding to Cas9 can be seen in the Cas9 hom samples, it was reassuring

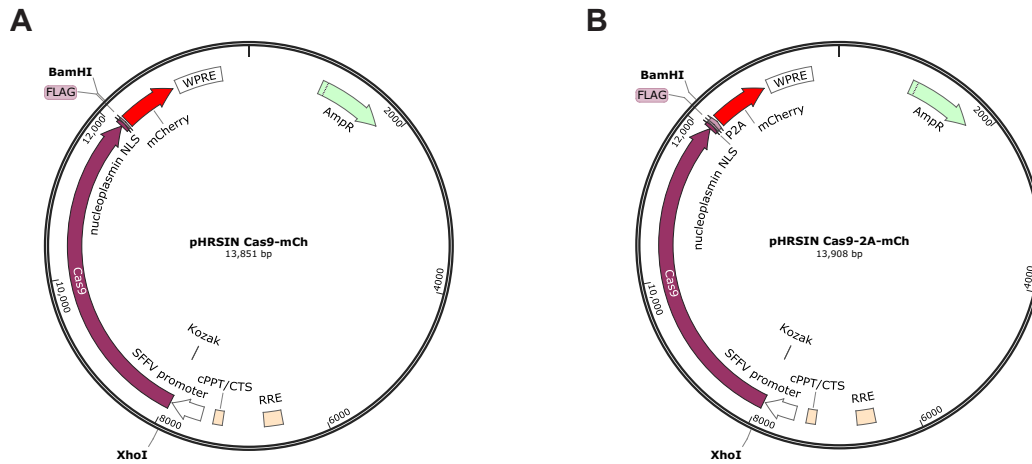


Fig. 6.4 **Final Cas9-mCh and Cas9-2A-mCh pHRSIN plasmids maps.** Two Cas9-containing pHRSIN-mCh plasmids were produced: **A** One plasmid with Cas9 directly fused to mCherry. **B** A second plasmid where Cas9 and mCherry are separated by a P2A sequence. Plasmid maps were created with *snappgene*. RRE = rev response element, cPPT = central polypurine tract, SFV = spleen focus forming virus promoter, Cas9 = CRISPR-associated protein 9, NLS = nuclear localisation sequence, Flag = flag octapeptide tag, P2A = P2A self-cleaving peptide, WPRE = woodchuck hepatitis virus post-transcriptional regulatory element, AmpR = ampicillin resistance gene.

that these correspond to the same molecular weight as the lower band in the Cas9-2A-mCh lentivirus transduced samples (the version of Cas9 where mCherry was cleaved from Cas9). However, using lentivirus from the same stock did not result in mCherry positive hCTL (data not shown), again indicating difficulty in transducing this cell type.

6.2.3 Transduction of human T cells with Cas9-2A-mCh lentivirus

Since the Cas9-2A-mCh lentivirus worked on various cell lines, but not on primary hCTL, I set out to determine the titre of the lentivirus produced. I determined the lentivirus viral titre on Jurkat cells (Figure 6.7A), as an easy-to-transduce cell type, that will therefore provide an accurate representation of the viral titre, but is also related to primary human T cells. This showed that my standard lentiviral production protocol produced Cas9-2A-mCh lentivirus at a high titre (1.8×10^7 TU/ml).

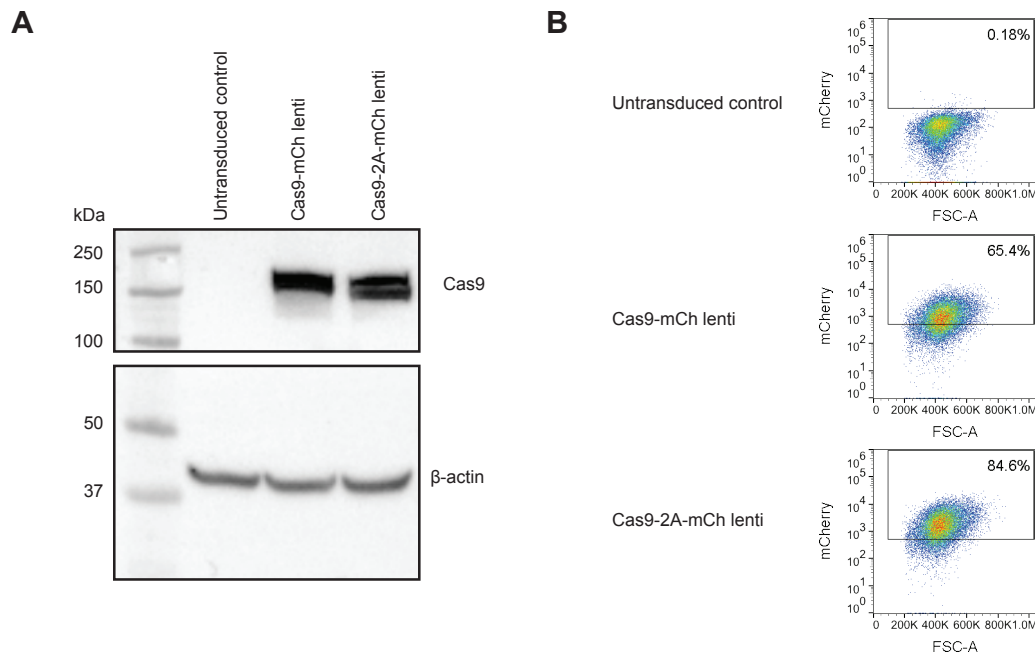


Fig. 6.5 Transduction of P815 cells with Cas9-mCh and Cas9-2A-mCh lentivirus. **A** WB showing Cas9 expression after transduction of P815 cells with the Cas9-mCh or Cas9-2A-mCh lentivirus. **B** Flow cytometry plots showing the expression of mCherry-positive P815s after transduction with Cas9-mCh or the Cas9-2A-mCh lentivirus.

Next, I tried to optimise transduction efficiency in primary human CTL. I normally included protamine sulfate in transduction experiments. Protamine sulfate is a polycationic polymer that neutralises the charge repulsion between the viral membrane and the plasma membrane of the cell and has been shown to enhance transduction efficiencies in human T cells (Cornetta and Anderson, 1989). Another commercially available reagent, the poloxamer syneronic F108, also known as lentiboost, is known to enhance transduction efficiency via a different mechanism. Lentiboost interacts with membranes and increases their permeability (Höfig et al., 2012). A study comparing transduction efficiencies in mouse CD4 and CD8 T cells showed lentiboost performs better than protamine sulfate (Delville et al., 2018). Encouragingly, comparing transduction efficiencies between samples transduced with the 'empty' pHRSIN-mCh lentivirus showed that transduction efficiency was higher in the presence of lentiboost in comparison to protamine sulfate (Figure 6.7B). All of the Cas9-2A-mCh lentivirus remaining from the viral titration was aliquoted between cells derived from three different HDs, meaning that these cells were only transduced at a low MOI of 1.17. As observed with the 'empty' pHRSIN-mCh lentivirus, transduction with the pHRSIN Cas9-2A-mCh lentivirus in the presence of lentiboost resulted in a higher transduction efficiency

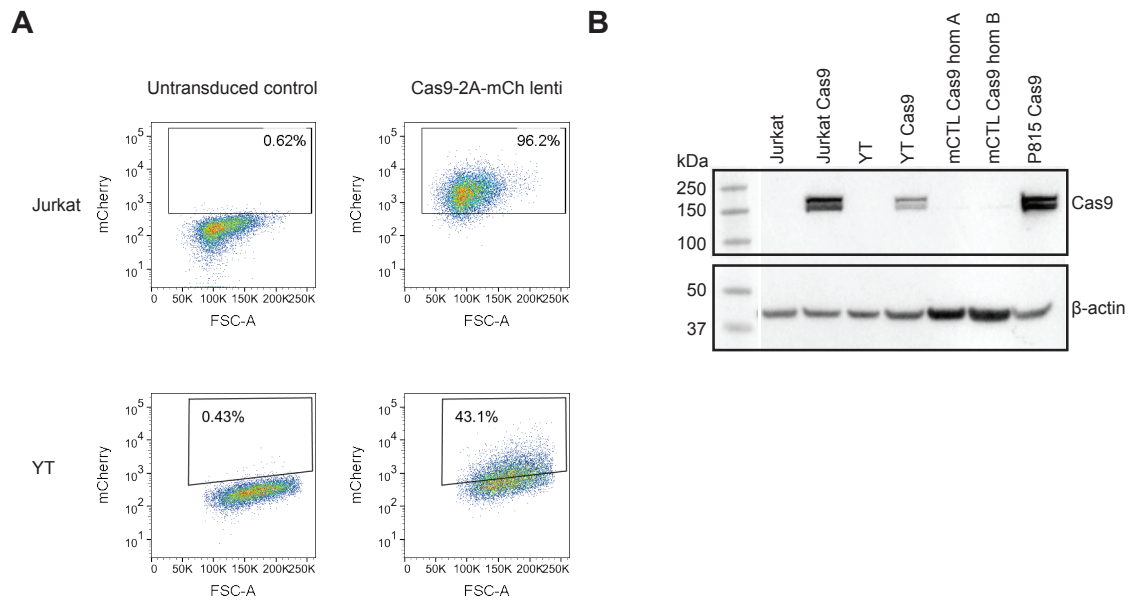


Fig. 6.6 Transduction of Jurkat and YT cell lines with Cas9-2A-mCh lentivirus. **A** Flow cytometry plots showing the expression of mCherry in YTs and Jurkat cells after transduction with the Cas9-2A-mCh lentivirus. **B** WB comparing Cas9 expression in lysates derived from Cas9 hom mCTL to lysates derived from YTs, Jurkat cells and P815s transduced with the Cas9-2A-mCh lentivirus.

in comparison to transduction with protamine sulfate (Figure 6.7B,C). While transduction efficiency was variable in cells from different HDs, up to 17% mCherry-positive cells were achieved after transduction with Cas-2A-mCh lentivirus in the presence of lentiboost (Figure 6.7D). FACS was used to isolate the mCherry-positive population, however, the cells did not expand further after sorting. This indicated that in addition to the challenge of low transduction efficiency with the large Cas9-2A-mCh lentivirus, sorting primary human T cells provided another hurdle to using the lentiviral CRISPR approach in primary human T cells.

6.2.4 Nucleofection of primary human T cells

As an alternative approach that does not require sorting, I tested the CRISPR approach using RNPs, as described in chapter 3, in hCTLs. This approach has been successfully used by others, mostly in human CD4 T cells (Hultquist et al., 2016; Roth et al., 2018; Rupp et al., 2017; Schumann et al., 2015). As hCTL had not previously been successfully nucleofected in our lab, I initially compared the nucleofection efficiency achieved with two different machines (the neon from ThermoFisher Scientific and the 4D from Lonza). When

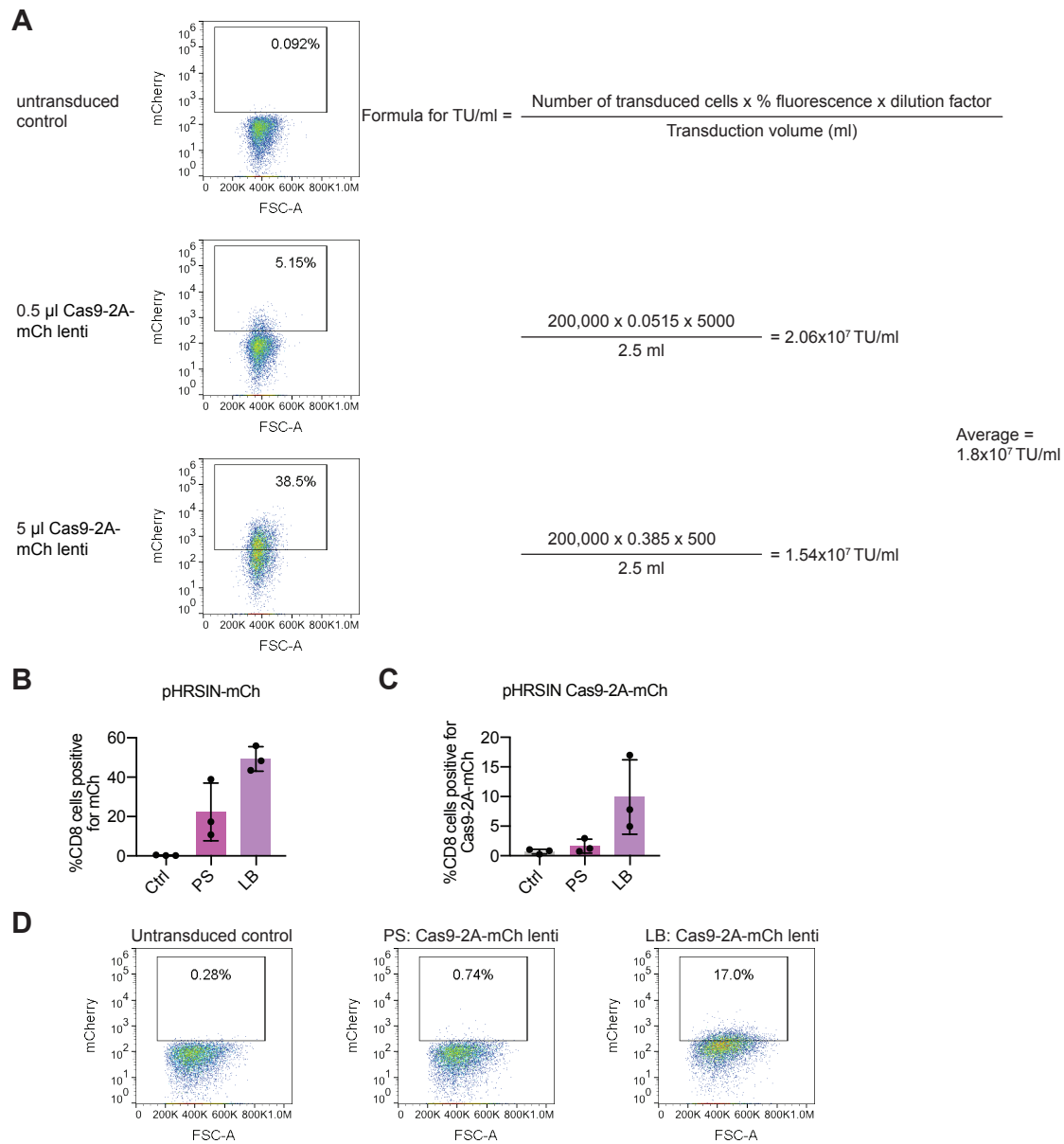


Fig. 6.7 Transduction of human T cells with Cas9-2A-mCh lentivirus. **A** Determination of viral titre of the Cas9-2A-mCh lentivirus by transducing Jurkat cells. **B** mCherry expression in primary hCTL transduced with pHRSIN-mCh lentivirus using protamine sulfate (PS) or lentiboost (LB) as transduction enhancers. Bar graphs show the mean \pm SD. **C** mCherry expression in primary hCTL transduced with pHRSIN-Cas9-2A-mCh lentivirus at MOI of 1.17 using PS or LB as transduction enhancers. The bar graphs show the average of 3 independent experiments, error bars show the SD. **D** Flow cytometry plots showing mCherry expression in response to transduction of hCTL derived from the same HD at MOI of 1.17 in the presence of PS or LB reagents. LB = lentiboost. PS = protamine sulfate.

nucleofecting a plasmid encoding lifeact-EGFP the nucleofection efficiency achieved with the two machines was similar, showing an average nucleofection efficiency of 51.38% (neon) and 56.52% (4D) after one day (Figure 6.8). The fluorescent signal was maintained until day 4 and decreased by day 7 after nucleofection (Figure 6.8).

To test the RNP CRISPR system I used synthetic crRNA reagents targeting the human *CD2* gene, co-nucleofected alongside tracrRNA and Cas9 protein as established for mCTL in chapter 3. *CD2* was targeted as it encodes a cell surface protein that is easily monitored by flow cytometry. I only used 1-1.5 million cells per nucleofection and scaled down the CRISPR reagents accordingly (e.g. in chapter 3 I used 5 μ g per crRNA when nucleofecting 5 million cells, therefore I used 1 μ g per crRNA for 1 million cells). A decrease in CD2 levels could be observed 4 days after nucleofection (Figure 6.9). Strikingly, the percentage of cells that lost surface expression of CD2 was higher in samples that were nucleofected with the neon nucleofection system (n=6, p<0.001 at day 4, unpaired t-test with Welch's correction). Importantly, the KO was stably maintained until the last time point measured (one month after nucleofection). This confirmed the great potential of using hCTL over mCTL to produce stable KOs that are long-lived in tissue culture.

6.2.5 Comparing CRISPR KO efficiency with stable and transient Cas9 expression

Finally, I asked how the stable expression of Cas9 achieved through using the Cas9-2A-mCh lentivirus compared to the transient nucleofection of Cas9-RNP complexes in terms of CRISPR efficiency. Jurkat cells were used that were either untransduced or between 90-100% positive for Cas9-2A-mCh after transduction. While Jurkat cells were nucleofected with Cas9 protein, tracrRNA and crRNAs targeting *CD2*, Cas9-2A-mCh-transduced Jurkat cells were only nucleofected with tracrRNA and crRNAs targeting *CD2*. The percentage of CD2 expression at the cell surface was measured at day 5 and day 14 after nucleofection. Initially, I used the same number of cells and same concentration of reagents previously used for *CD2* CRISPR in human T cells. However, a convincing decrease in CD2 levels was not observed at day 5 or day 14 post nucleofection (Figure 6.10A). Following the manufacturer's protocol, I scaled down the number of cells nucleofected from 1 million (using cuvettes for nucleofection) to 0.2 million (using 16-well strips for nucleofection) while keeping the amount of CRISPR reagent the same, thereby increasing the reagent-to-cell ratio. This showed successful CRISPR-mediated loss of CD2 protein cell surface expression in transient

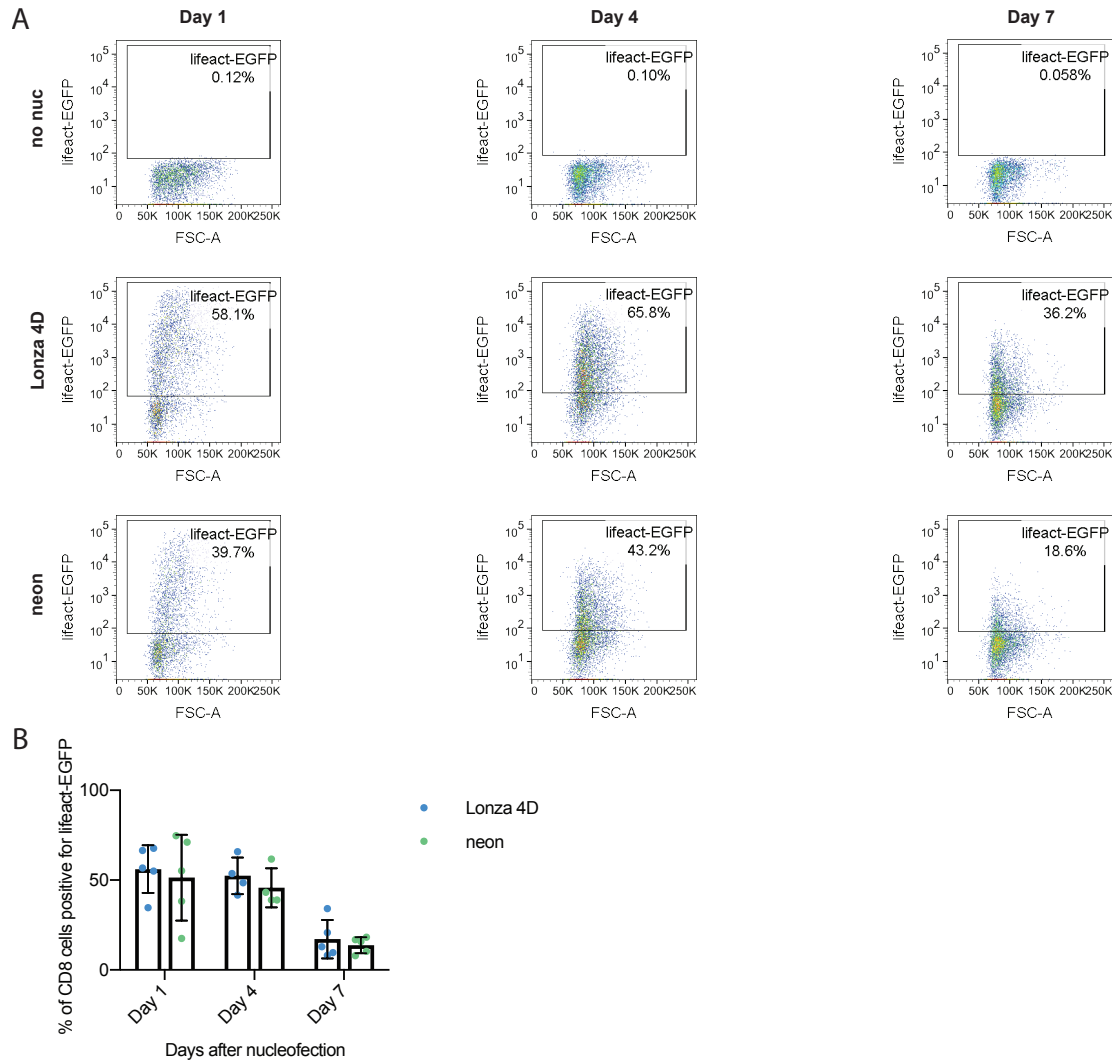


Fig. 6.8 Nucleofection of human T cells with lifeact-EGFP. PBMCs were isolated from buffycoat and activated with 5 $\mu\text{g/ml}$ PHA. At day 3 post activation, 1.5 million cells were nucleofected with 2 μg lifeact-EGFP plasmid using the Lonza 4D or neon nucleofection machines. The percentage of cells positive for lifeact-EGFP was determined by flow cytometry at day 1, 4 and 7 post nucleofection. **A** Representative flow cytometry plots. **B** Average lifeact-EGFP expression measured by flow cytometry at day 1, 4 and 7 post nucleofection. The bar graphs show the average of 5 independent experiments, error bars show the SD. no nuc = no nucleofection control.

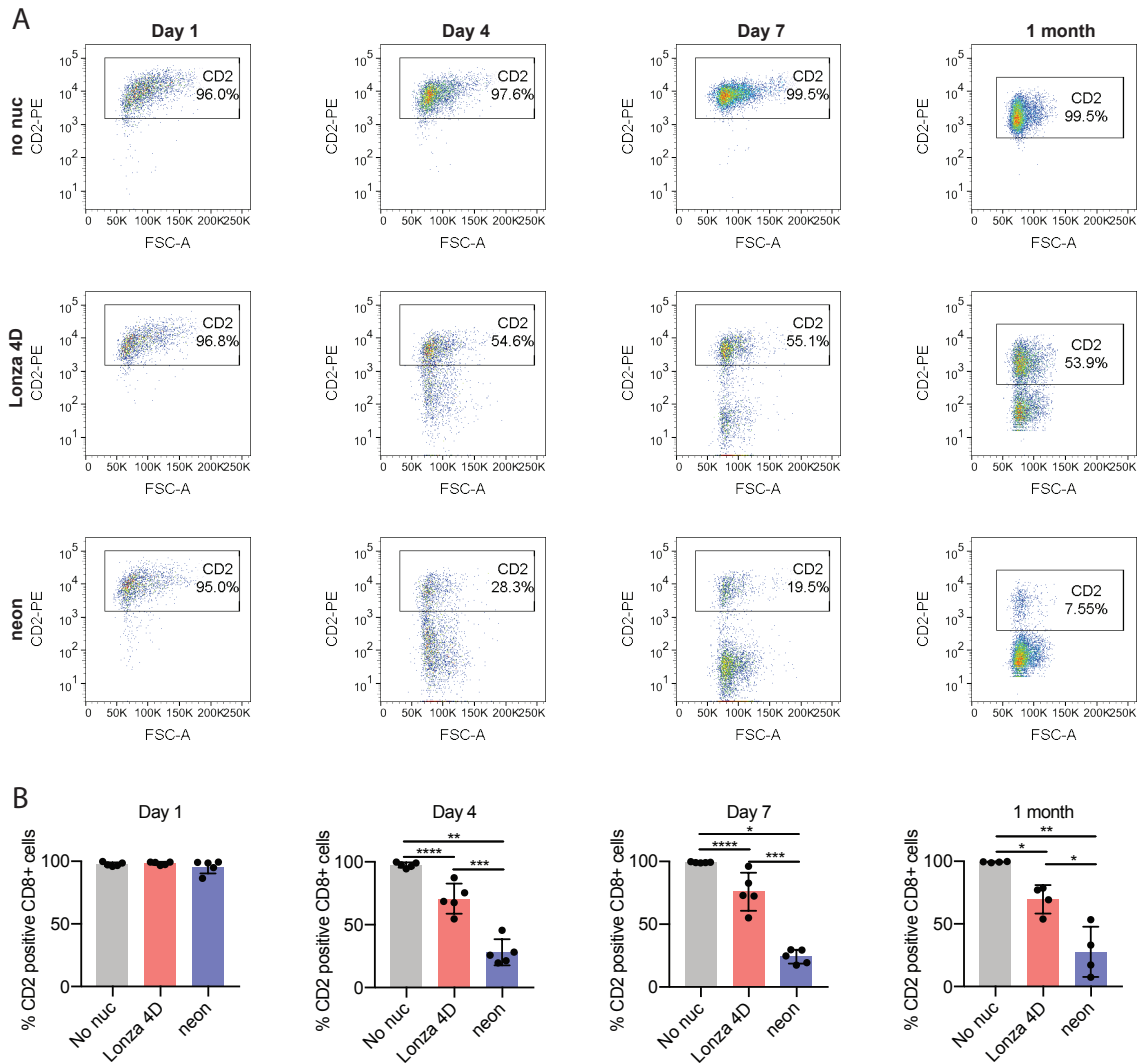


Fig. 6.9 Targeting CD2 by CRISPR using Cas9-RNP in human T cells. PBMCs were isolated from buffycoat and stimulated with 5 $\mu\text{g/ml}$ PHA for three days prior to nucleofection. 1-1.5 million cells per condition were nucleofected with Cas9-RNPs targeting CD2. The Lonza 4D and neon nucleofection machines were tested in parallel. **A** Representative flow cytometry plots showing the percentage of cells positive for cell surface CD2 at day 1, 4 and 7 or one month after nucleofection. **B** Average CD2 cell surface expression measured by flow cytometry at day 1, 4 and 7 ($n=5$ independent experiments) and one month post nucleofection ($n=4$ independent experiments), * $p<0.05$, ** $p<0.01$, *** $p<0.001$, **** $p<0.0001$, unpaired t -test with Welch's correction. Bar graphs show the mean \pm SD, no nuc = no nucleofection control.

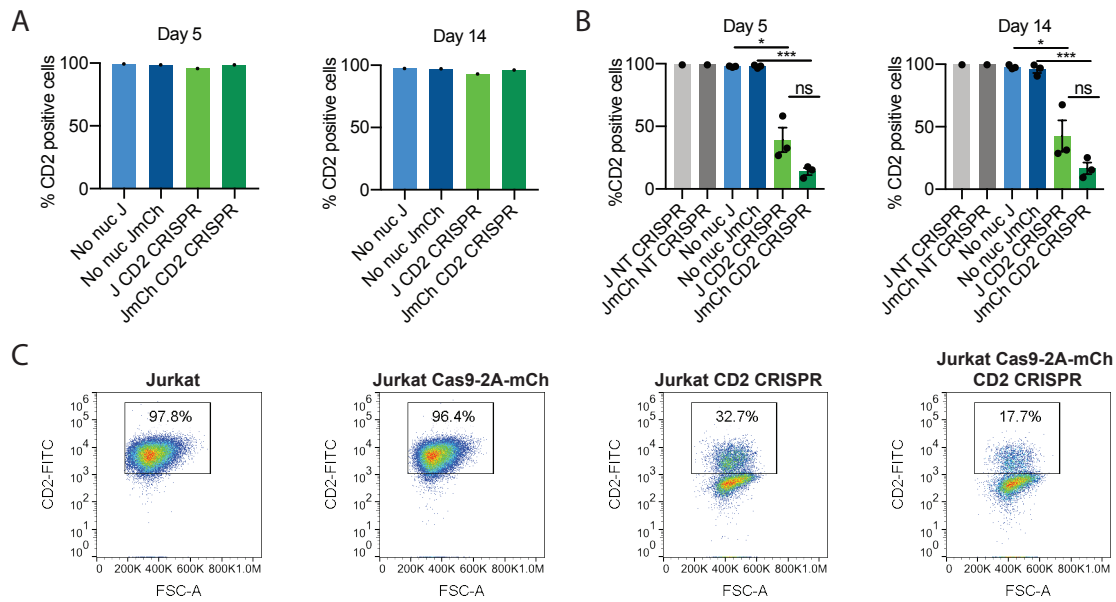


Fig. 6.10 CRISPR KO efficiency with transient and stable Cas9 expression targeting CD2 in Jurkat cells. **A** 1 million Jurkat cells were nucleofected with 1 μ g per CD2 crRNA (3 crRNAs in total), 3 μ g tracrRNA and 2 μ g Cas9 protein using the Lonza 4D nucleofection machine. CD2 cell surface expression was measured by flow cytometry at day 5 and day 14 post nucleofection, $n=1$. **B** 0.2 million Jurkat cells were nucleofected with 1 μ g per CD2 crRNA (3 crRNAs in total), 3 μ g tracrRNA and 2 μ g Cas9 protein using the Lonza 4D nucleofection machine. CD2 cell surface expression was measured by flow cytometry at day 5 and day 14 post nucleofection. NT samples: $n=1$, No nuc and CD2 CRISPR samples: $n=3$ independent experiments, $*p<0.05$, $***p<0.001$, unpaired t -test with Welch's correction. Bar graphs show the mean \pm SD. **C** Representative flow cytometry plots showing CD2 cell surface expression at day 5 post nucleofection. J=Jurkat, JmCh = Jurkat Cas9-2A-mCh, NT = non-targeting, no nuc = no nucleofection control, ns = not significant.

($n=3$, $p<0.05$ at day 5, unpaired t -test with Welch's correction) and stable ($n=3$, $p<0.001$ at day 5, unpaired t -test with Welch's correction) Cas9 samples (Figure 6.10B,C). Similar results were achieved when targeting the gene encoding the cell surface protein B2M (Figure 6.11A,B) ($n=3$, $p<0.01$ for transient Cas9, $p<0.001$ for stable Cas9, unpaired t -test with Welch's correction). This confirmed that the Cas9-2A-mCh construct encoded functional Cas9 protein. For both genetic targets, the sample with stable lentiviral transduction of Cas9 showed a trend towards better CRISPR KO efficiency in comparison to the respective Cas9 protein nucleofected sample, however, this trend was not statistically significant (Figures 6.10 and 6.11).

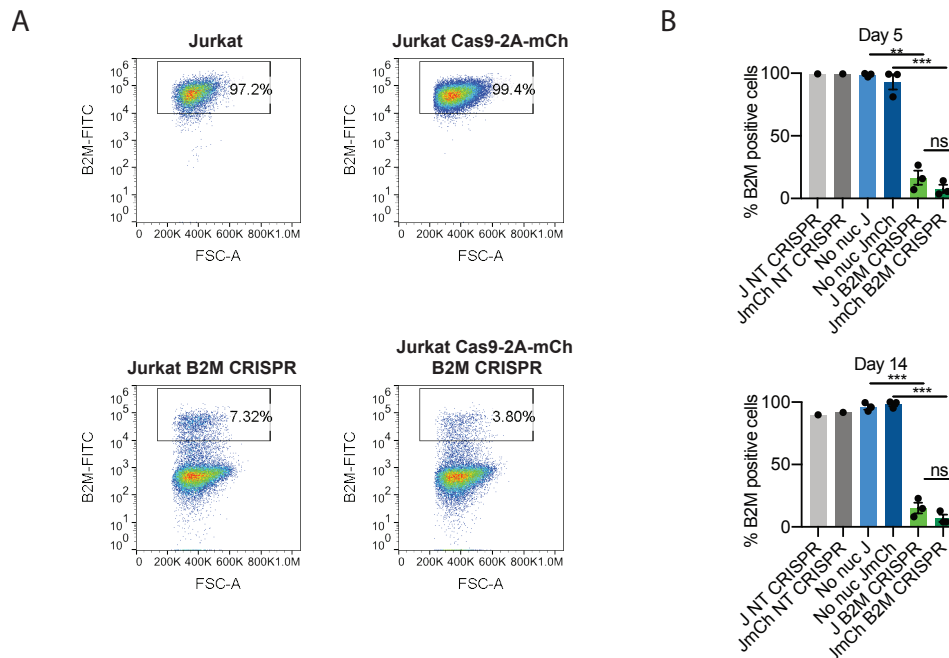


Fig. 6.11 CRISPR KO efficiency with transient and stable Cas9 expression targeting B2M in Jurkat cells. 0.2 million Jurkat cells were nucleofected with 1 μ g per B2M crRNA (3 crRNAs in total), 3 μ g tracrRNA and 2 μ g Cas9 protein using the Lonza 4D nucleofection machine. B2M cell surface expression was measured by flow cytometry at day 5 and day 14 post nucleofection. **A** Representative flow cytometry plots showing B2M cell surface expression at day 5 post nucleofection. **B** Bar graphs showing the average B2M cell surface expression at day 5 and day 14 post nucleofection, NT samples: $n=1$, No nuc and B2M CRISPR samples: $n=3$ independent experiments, $**p<0.01$, $***p<0.001$, unpaired t -test with Welch's correction. Bar graphs show the mean \pm SD. J=Jurkat, JmCh = Jurkat Cas9-2A-mCh, NT = non-targeting, no nuc = no nucleofection control, ns = not significant.

6.3 Discussion

The blasticidin selection time and concentration required to select for a transduced population can vary greatly between cell types. Too much antibiotic kills cells including transduced cells, not enough drug will result in untransduced cells being left in the population (Doench, 2017). 5 μ g/ml blasticidin was the lowest concentration that seemed to kill all untransduced cells, although even 1 μ g/ml blasticidin had a stark effect on the FSC/SSC profile of hCTLs after 15 days of treatment (Figure 6.1). While transduction of hCTL with the Cas9-Blast lentivirus appeared to be successful by PCR, only few cells survived the treatment with 5 μ g/ml blasticidin (Figure 6.2), indicating that this blasticidin concentration may have been

too high, killing everything including transduced cells. On top of this, low transduction efficiency, as indicated by the WB and PCR results (Figure 6.2), likely also contributed to the unsuccessful selection of Cas9-expressing cells. In agreement with my results, a published study using a lentivirus encoding a puromycin resistance gene alongside Cas9 observed immense cell death (>90%) upon antibiotic selection (Legut et al., 2018).

In order to be able to visualise transduction efficiency more clearly than by blasticidin selection, I cloned the *Cas9* gene into a lentiviral vector expressing the fluorescent protein mCherry (Figures 6.3 and 6.4). Two versions of the vector were produced, one where Cas9 was directly fused to mCherry and another where Cas9 and mCherry were separated by a self-cleaving 2A peptide (Figure 6.4). Using the resulting vector to produce lentivirus resulted in successful transduction of P815, YT and Jurkat cell lines (Figures 6.5 and 6.6). Due to concerns that directly fusing Cas9 to mCherry might affect its function the Cas9-2A-mCh lentivirus was used subsequently.

2A peptides are used to co-express two genes in one mRNA transcript, which are then cleaved co-translationally (Kim et al., 2011). While 2A peptides have been identified from several different viruses, a study showed that the P2A peptide, derived from porcine teschovirus, has the highest cleavage efficiency in human cell lines in comparison to 2A peptides derived from three other viruses (Kim et al., 2011). However, in this chapter there was only partial cleavage between Cas9 and mCherry in all cells tested, as shown by two bands being detected when blotting for Cas9 (Figures 6.5 and 6.6). The lower molecular weight band likely corresponded to Cas9 cleaved from mCherry and the higher molecular weight band to Cas9 still fused to mCherry. I would have expected higher cleavage efficiency of the P2A peptide based on the published data (Kim et al., 2011). This means that the Cas9 pool in the Cas9-2A-mCh transduced samples is a heterogenous population of Cas9 cleaved from mCherry and Cas9 fused to mCherry. Therefore it was crucial to confirm that this mixed population of Cas9 is functional as fusion to mCherry could affect its activity. The results obtained with Cas9-2A-mCh Jurkat cells showed high KO efficiency when targeting *B2M* and *CD2* using CRISPR (Figures 6.10 and 6.11), indicating that the Cas9-2A-mCh cleaved and uncleaved products are both functional.

It is known that as vector length increases, viral titre decreased (Ramezani and Hawley, 2002), meaning that viruses containing a large insert, such as Cas9, are likely to have a relatively low titre (Doench, 2017). Here I managed to produce the Cas9-2A-mCh lentivirus at a high viral titre (Figure 6.7), however, transduction of human T cells with Cas9-2A-mCh

lentivirus was still challenging, and much less efficient than transduction of Jurkat, YT or P815 cell lines. Lentiboost proved to be a better transduction enhancer than protamine sulfate, yielding 17% transduction efficiency with the Cas9-2A-mCh lentivirus in cells derived from one HD (Figure 6.7). However, the fluorescence level in the population positive for Cas-2A-mCh was low, which could indicate a low level of Cas9 expression (Figure 6.7).

A recently published study also reported low transduction efficiency when transducing T cells with lentivirus encoding Cas9-2A-GFP, obtaining 5% GFP-positive cells (Seki and Rutz, 2018). They noted a low level of GFP fluorescence as well, and concluded that the lentiviral approach is inefficient (Seki and Rutz, 2018). Notably, I achieved up to 17% transduction efficiency when using the Cas9-2A-mCh lentivirus at a low MOI of 1.17. It would therefore be worthwhile to try to transduce human T cells at a higher MOI to see if the percentage of transduced cells could be increased further.

Meanwhile, I successfully used the Cas9-RNP nucleofection approach to target *CD2* in human T cells (Figure 6.9). Throughout my PhD project, several studies have been published using this approach, some have used the 4D nucleofector (Hultquist et al., 2016; Roth et al., 2018; Rupp et al., 2017) and others the neon nucleofection machine (Gundry et al., 2016; Schumann et al., 2015). While the two machines seemed similarly efficient when nucleofecting a DNA plasmid encoding lifeact-EGFP (Figure 6.8), nucleofection with the neon resulted in higher *CD2* KO efficiency (Figure 6.9). This may be due to differences between the nucleofection solutions or nucleofection pulses used, which can affect cell permeability and perhaps even Cas9-RNP complex stability. On average, I achieved a 71.88% decrease in *CD2* expression when using the neon nucleofection machine, but only a 29.28% decrease in *CD2* with the 4D nucleofector at day 4 post nucleofection (n=5, p<0.001, unpaired t-test with Welch's correction, Figure 6.9).

Finally, I asked if CRISPR efficiency differed when using transient Cas9 expression (Cas9-RNP nucleofection approach) or stable Cas9 expression (transduction with Cas9 lentivirus) in Jurkat cells. Surprisingly, the initial attempt to nucleofect Jurkat cells with *CD2* CRISPR components was unsuccessful (Figure 6.10). Successful CRISPR-mediated KO of *CD2* and *B2M* was achieved when scaling down the number of cells used (Figures 6.10 and 6.11), indicating that a higher reagent-to-cell concentration was needed for CRISPR in Jurkat cells than in hCTL. Jurkat cells may have an abnormal karyotype, and therefore potentially more than two copies of the *CD2* gene, which could explain the requirement for more CRISPR reagents to cut all alleles. In agreement with this, some published studies indicated

that Jurkat cells may have a hypotetraploid genome (Cheng and Haas, 1990; Snow and Judd, 1987). Targeting *CD2* and *B2M* in Cas9-2A-mCh-transduced and untransduced Jurkat cells indicated that the CRISPR efficiency achieved with stable and transient Cas9 expression was comparable. A non-significant trend towards better KO efficiency was observed with stable Cas9 expression. However, this may just be due to Cas9 protein being limited by nucleofection efficiency, while 90-100% of the Cas9-2A-mCh-transduced Jurkat cells were expressing Cas9 according to mCherry expression measured by flow cytometry.

The Cas9-RNP approach is very useful to target specific genes or perform arrayed screens (see chapter 4). However, if complete KOs are desired, it might be worth transducing hCTL with Cas9 lentivirus at a higher MOI and further optimising hCTL survival after sorting in order to generate hCTL that stably express Cas9. Subsequent transduction with a sgRNA-containing lentivirus would likely be more efficient due to the smaller insert size, allowing antibiotic selection and the generation of complete KOs. Stably expressing Cas9-hCTL would also open the possibility of a genome-wide screen in primary human T cells. Until recently, genome-wide screens had only been performed in cell lines related to primary T cells, such as Jurkat and CCRF-CEM cells (Park et al., 2017; Shang et al., 2018). Recently, a group took an alternative approach where they transduced primary human T cells with a lentiviral sgRNA library followed by nucleofection of Cas9 protein (Shifrut et al., 2018). The methods and reagents optimised in this chapter could be used to produce human T cells stably expressing Cas9. If a Cas9-pure population could be isolated, transduction with a genome-wide sgRNA lentiviral library would perhaps allow the unbiased pooled genome-wide screening approach in primary human T cells.

6.3.1 Summary and evaluation of aims

- Transduce hCTL with a lentivirus encoding Cas9 as well as antibiotic resistance or a fluorescent marker to be able to select successfully transduced cells.
 - Initially, hCTL were transduced with a lentivirus encoding Cas9 and antibiotic resistance to blasticidin. However, blasticidin selection was challenging due to low transduction efficiency. To obtain a direct readout of the transduction efficiency, Cas9 was cloned into a lentiviral vector that encodes a fluorescent marker (pHRSIN-mCh). This lentiviral vector has previously been used to transduce primary human hematopoietic cells (Demaison et al., 2002). I successfully used the resulting lentivirus to transduce Jurkat cells, YTs and P815s. Human T cell transduction proved more challenging due to low transduction efficiency with

such a large construct. Using an alternative transduction enhancer to protamine sulfate, lentiboost, improved transduction efficiency.

- Test nucleofection of hCTL and the transient Cas9-RNP CRISPR approach (optimised in chapter 3) in primary hCTL.
 - I tested two machines commonly used to nucleofect human T cells. At day 4 post nucleofection, *CD2* was knocked out in an average of 71.88% of cells using the neon machine and 29.28% of cells using the Lonza 4D nucleofection machine.
- Compare the stable (Cas9 lentivirus) and transient (Cas9-RNP) approaches in terms of CRISPR efficiency.
 - Using Jurkat cells I showed that the CRISPR efficiency was comparable when using stable or transient Cas9. Cells transduced with the Cas9 lentivirus showed a slight trend towards better KO efficiency when targeting *CD2* (averages from day 5: Jurkat: 60.77% KO, Jurkat Cas9-2A-mCh: 86.06% KO) and *B2M* (averages from day 5: Jurkat: 83.26% KO, Jurkat Cas9-2A-mCh: 92.05% KO).

